2-19-2016

Organotypic slice cultures containing the preBotzinger complex generate respiratory-like rhythms

Wiktor S. Phillips

Mikkel Herly

Jens C. Rekling

Christopher A. Del Negro
William & Mary

Recommended Citation

Phillips, Wiktor S.; Herly, Mikkel; Rekling, Jens C.; and Del Negro, Christopher A., Organotypic slice cultures containing the preBotzinger complex generate respiratory-like rhythms (2016). *Journal of Neurophysiology*, 115(2), 1063-1070.
10.1152/jn.00904.2015

J Neurophysiol 115: 1063–1070, 2016.
First published December 9, 2015; doi:10.1152/jn.00904.2015.

Organotypic slice cultures containing the preBötzinger complex generate respiratory-like rhythms

Wiktor S. Phillips,[1,2] Mikkel Herly,[1] Christopher A. Del Negro,[2] and Jens C. Rekling[1]
[1]*Department of Neuroscience and Pharmacology, University of Copenhagen, Copenhagen, Denmark; and* [2]*Department of Applied Science, The College of William and Mary, Williamsburg, Virginia*

Submitted 24 September 2015; accepted in final form 2 December 2015

Phillips WS, Herly M, Del Negro CA, Rekling JC. Organotypic slice cultures containing the preBötzinger complex generate respiratory-like rhythms. *J Neurophysiol* 115: 1063–1070, 2016. First published December 9, 2015; doi:10.1152/jn.00904.2015.—Study of acute brain stem slice preparations in vitro has advanced our understanding of the cellular and synaptic mechanisms of respiratory rhythm generation, but their inherent limitations preclude long-term manipulation and recording experiments. In the current study, we have developed an organotypic slice culture preparation containing the preBötzinger complex (preBötC), the core inspiratory rhythm generator of the ventrolateral brain stem. We measured bilateral synchronous network oscillations, using calcium-sensitive fluorescent dyes, in both ventrolateral (presumably the preBötC) and dorsomedial regions of slice cultures at 7–43 days in vitro. These calcium oscillations appear to be driven by periodic bursts of inspiratory neuronal activity, because whole cell recordings from ventrolateral neurons in culture revealed inspiratory-like drive potentials, and no oscillatory activity was detected from glial fibrillary associated protein-expressing astrocytes in cultures. Acute slices showed a burst frequency of 10.9 ± 4.2 bursts/min, which was not different from that of brain stem slice cultures (13.7 ± 10.6 bursts/min). However, slice cocultures that include two cerebellar explants placed along the dorsolateral border of the brainstem displayed up to 193% faster burst frequency (22.4 ± 8.3 bursts/min) and higher signal amplitude (340%) compared with acute slices. We conclude that preBötC-containing slice cultures retain inspiratory-like rhythmic function and therefore may facilitate lines of experimentation that involve extended incubation (e.g., genetic transfection or chronic drug exposure) while simultaneously being amenable to imaging and electrophysiology at cellular, synaptic, and network levels.

preBötzinger complex; breathing; respiration; central pattern generator; organotypic slice cultures; rhythmogenesis; rhythm generation

FOR NEARLY TWENTY-FIVE YEARS, investigators have employed acute transverse slice preparations containing the preBötzinger complex (preBötC) to probe the cellular and synaptic bases for respiratory rhythm generation in rodents (Feldman et al. 2013; Funk and Greer 2013; Smith et al. 1991). These "breathing slice" preparations retain sufficient circuitry from the respiratory medulla to spontaneously generate inspiratory-related rhythms and motor output, measurable via the hypoglossal (XII) cranial nerve root. Acute slices provide optimal access for electrophysiological, optical, and pharmacological experiments, which has helped define fundamental cellular and synaptic neural mechanisms underlying inspiratory rhythms as well as basic neuromodulatory mechanisms that influence network activity (Feldman et al. 2013; Funk and Greer 2013; Ramirez et al. 2012).

However, acute slices remain viable and rhythmically active for ~1 day (Funk and Greer 2013), which limits the scope of techniques that may be applied. Pharmacological assays are limited to time windows of several hours, which prohibit studies of chronic drug effects on respiratory network function. Furthermore, experiments that involve genetic manipulation or transfection require several days for protein expression and thus are impossible to perform using acute slices. It would therefore be advantageous to have an in vitro preparation that retains a functional preBötC for days or weeks, and facilitates genetic and pharmacological manipulation while retaining behaviorally relevant network activity that can be monitored and recorded with the ease offered by acute slices.

With the use of organotypic culturing techniques, partial slice preparations of the preBötC have been successfully maintained over multiweek periods (Hartelt et al. 2008). These slice cultures, cut 250 μm thick, preserve some rhythmogenic function but contain only a fraction of the preBötC neurons normally captured in 400- to 700-μm-thick breathing slices (Funk and Greer 2013). Hartelt et al. recorded rhythmic low-frequency action potential bursts in some cells but did not analyze whether coordinated patterns of network activity were generated in their cultures. Thus a culture preparation that retains the preBötC rhythmogenic core bilaterally, throughout its anterior-posterior extent, which typifies acute rhythmically active slice preparations, has not yet been described.

In this article we present a novel slice preparation that retains the preBötC bilaterally using both the Stoppini membrane method and the Gähwiler roller-drum method of organotypic slice culturing (Gahwiler 1981; Stoppini et al. 1991). This new culture preparation generates synchronized network activity bilaterally in the ventrolateral, preBötC-related regions of the slice, analogous to rhythms in acute slice preparations. The preparation shows spontaneous rhythm over several weeks of culturing and flattens out, which improves the quality of optical imaging at the cellular and network level. Furthermore the neurons are accessible for whole cell patch clamping, meaning that both network activity and individual neurons can be selectively recorded from and perturbed using methods already established in the acute slice preparation.

MATERIALS AND METHODS

Ethical approval. The Department of Experimental Medicine at the Panum Institute approved all experiments and procedures according to protocols laid out by Danish Ministry of Justice and the Danish National Committee for Ethics in Animal Research.

Address for reprint requests and other correspondence: J. C. Rekling, Dept. of Neuroscience and Pharmacology, Univ. of Copenhagen, Panum Institute 33.3.84, Blegdamsvej 3, DK-2200 Copenhagen N, Denmark (e-mail: jrekling@sund.ku.dk).

Organotypic slice cultures. U.S. Naval Medical Research Institute (NMRI) mice postnatal ages 0.5–5.5 days were anesthetized with isoflurane and immediately dissected in sterile-filtered chilled artificial cerebrospinal fluid (ACSF) containing (in mM) 184 glycerol, 2.5 KCl, 1.2 NaH_2PO_4, 30 $NaHCO_3$, 20 HEPES, 25 D-glucose, 5 sodium ascorbate, 2 thiourea, 3 sodium pyruvate, 10 $MgSO_4$, and 0.5 $CaCl_2$; pH 7.3, equilibrated by bubbling with carbogen (95% O_2 and 5% CO_2). We cut transverse slices of the brain stem, 400 μm in thickness, at the level of the preBötC on a vibratome (Thermo Scientific Microm 650V; Waltham, MA) as described by newborn mouse atlases of the brain stem (Ruangkittisakul et al. 2011, 2014). Additionally, we often retained 400-μm-thick parasagittal slices of the cerebellum from the same mouse brain for co-culturing. For Stoppini-type cultures, transverse brain stem slices were placed onto semiporous culture well inserts (Millipore PIC03050; Darmstadt, Germany) with cerebellar explants cocultured along their dorsolateral borders. Mounted preparations were maintained in sterile-filtered organotypic culture medium containing 50% Eagle's MEM with Earle's salts, 25% Hank's balanced salt solution, 25% heat-inactivated horse serum, 2 mM glutamine, 200 U/ml penicillin, 5 μg/ml streptomycin, 10 mM HEPES, and an additional 3.6 mM D-glucose. The cultures were treated with 10 μM MK-801, an NMDA receptor antagonist, for the first 3 days in vitro. Fresh culture medium was supplied every 48 h thereafter until experimentation. These slices were then kept in a sterile humidified incubator at 35°C and atmospheric CO_2 concentrations during incubation.

We prepared some cultures according to the roller-drum technique, wherein the slices were placed on a coverslip embedded in citrated chicken plasma (Sigma-Aldrich, St. Louis, MO) that was then coagulated by adding a drop of 100–150 U/μl thrombin (Sigma-Aldrich). The cultures were kept in sealed plastic tubes (flat bottom; NUNC Thermo Scientific, Waltham MA) and placed in a rotating roller drum (15 revolutions/h) at 35°C in humidified air. All procedures were performed in a sterile work environment within a Class 1 biosafety cabinet. The success rate in obtaining oscillating cultures depended in particular on the dissection experience and skill of experimenter, and approached 100% after ~3 mo of training.

The thickness of the cultures was measured in counterstained sections using a Zeiss Axiolab microscope. The culture was drop fixed overnight in 4% paraformaldehyde, washed in Sørensen's phosphate buffer (0.1 M), dehydrated with increasing ethanol, embedded in Epon (EMBed-812; Electron Microscopy Sciences, Hatfield, PA), cut in 3-μm sections at a 90° angle relative to the surface on a microtome, counterstained with 0.1% toluidine (Sigma-Aldrich), and mounted with Eukitt mounting medium (Sigma-Aldrich).

Glial fibrillary acidic protein-labeled mice. Mice expressing enhanced green fluorescent protein (EGFP) under the promoter of glial fibrillary acidic protein [GFAP; line Tgn(hgFAPEGEP) GFEC 335] were kindly provided by Prof. Frank Kirchhoff (University of Saarland, Homburg, Germany) (Lalo et al. 2006).

Electroporation. Glass micropipettes were pulled from filamented capillary glass (outer diameter 1.5 mm, inner diameter 0.86 mm; Harvard Apparatus, Holliston, MA) using a PUL-100 micropipette puller (World Precision Instruments, Sarasota, FL), giving a tip diameter of 1–3 μm. Pipettes were filled with 1% biocytin, 1 M KCl, and 0.126 M Tris, which were placed in the slice culture, and positive current was applied in 50-ms pulses of 200 μA at 2 Hz for 10 min. Current pulses were generated by a stimulus isolation unit gated by a waveform generator (IsoFlex and Master-8; A.M.P.I., Jerusalem, Israel).

Calcium imaging and peptidergic compounds. Loading solutions for membrane-permeable calcium indicators were prepared by combining 30 μl of a 10 mM stock solution containing either fluo-8 AM in DMSO (AAT Bioquest, Sunnyvale, CA) or Asante calcium red AM in DMSO (TEFLabs, Austin, TX) with 3.5 μl of cremophore EL (Fluka, St. Louis, MO) and 7.5 μl of 20% pluronic acid in DMSO (AAT Bioquest). These 41 μl of dye solution were then dissolved in 1.5 ml of a standard ACSF containing 10 μM MK-571 (an ATP-binding cassette transporter blocker that improves calcium indicator dye uptake; Manzini et al. 2008). The ACSF consisted of (in mM) 129 NaCl, 3 KCl, 25 $NaHCO_3$, 5 KH_2PO_4, 30 D-glucose, 0.7 $CaCl_2$, 0.4 $MgSO_4$, 100 mM D-mannitol, which was aerated by bubbling with carbogen (95% O_2 and 5% CO_2) at room temperature. The final fluo-8 AM (or Asante calcium red) concentration was 20 μM. Slice cultures were submerged in bubbled loading solution for 30–60 min before recording began.

Fluorescent calcium activity was recorded in the slice culture using a stereo microscope (Leica MZ16 FA; Wetzlar, Germany) 30 min after the preparation was placed in a 2-ml recording chamber at 29°C and perfused at 2 ml/min with preheated oxygenated ACSF. Light-emitting diodes (LEDs; HLV series; CCS LED Spotlight, Kyoto, Japan) and a metal-halide light source (Leica EL6000) illuminated the preparation. Appropriate filter sets for green fluorescence (Leica GFP3: excitation bandpass 450–490 nm and emission bandpass 500–575 nm) were inserted in the light path for fluorescence imaging. Time series acquisition was performed with an electron-multiplying charge-coupled device camera (LucaEM S DL-658M; Andor Technology, Belfast, UK) at 10–129 Hz, controlled by SOLIS software (Andor Technology).

For cellular level fluorescence detection, a metal halide light source (PhotoFluor II; 89 North, Burlington, VT) or an LED light source (M470L2; Thorlabs, Newton, NJ) was coupled to a fixed-stage upright microscope via a liquid light guide and appropriate optical filters (for fluo-8 AM, a modified Olympus U-MWIB set: excitation 457–487 nm, dichroic mirror 505 nm, emission 515–550 nm; for Asante calcium red AM, an Olympus U-MWIG2 set: excitation 520–550 nm, dichroic mirror 565 nm, emission BA580IF nm). Images were captured by an sCMOS camera (Neo DC-152Q; Andor Technology) controlled by the SOLIS software (Andor Technology). Imaging protocols employed ×10 (NA 0.3), ×20 (NA 0.5), ×40 (NA 0.8), and ×63 (NA 0.95) water-immersion objectives. Time series images were acquired at 10–50 frames/s.

The NK1-receptor agonist substance P acetate salt hydrate (SP) and μ-opioid agonist [D-Ala^2, N-Me-Phe^4, Gly^5-ol]-enkephalin acetate salt (DAMGO; Sigma-Aldrich) were dissolved in water and further diluted in ASCF to give final concentrations of 500 nM and 1 μM, respectively. The effect of SP and DAMGO on burst frequency was tested in cumulative dosing measuring burst frequency over 20-s image stack in the control, 10 min of bath-applied substance P, and 10 min of SP plus DAMGO.

Whole cell patch clamp. Patch recordings employed an AxoClamp 2B amplifier (Molecular Devices, Sunnyvale, CA) and ROE-200 micromanipulators (Sutter Instruments, Novato, CA). Glass patch pipettes were pulled as described above to a tip resistance of 9–11 MΩ. Pipettes were loaded with a patch solution containing (in mM) 165 potassium D-gluconate, 10 NaCl, 0.5 $MgCl_2$, 10 HEPES, 0.4 GTP, 4 ATP, and 0.5 EGTA, pH 7.3, and then visually guided to target cells using a fixed-stage upright microscope (modified Olympus BX51) with a ×63 (NA 0.95) objective. Data were digitally acquired at 20 kHz. Rhythmically active neurons were first recorded with the minimum necessary current bias to achieve stable activity with little spontaneous firing during interburst intervals.

Analysis and statistics. Optical and electrophysiological data were analyzed offline using Igor Pro v. 6.36 (Wavemetrics, Lake Oswego, OR), Clampex 10.3 (Molecular Devices), and ImageJ v. 1.49 (Schneider et al. 2012). Change in fluorescence over baseline fluorescence intensity ($\Delta F/F_0$) was calculated using a moving Z projection that finds minimum values of fluorescence across consecutive 1-s time windows throughout an image stack. The 1-s running average, uniquely calculated for each individual frame, was subtracted from it throughout the time series to isolate fast calcium fluctuations from background fluorescence. Image stacks were then Kalman filtered to reduce noise and pseudocolored ("rainbow" RGB look-up table: red, maximum values of ΔF; green, medium values of ΔF; blue, minimum

values of ΔF). Pixels were binned (mean of adjacent 2 × 2–10 × 10 points) and brightness and contrast were enhanced using ImageJ. In some experiments, regions of interest (ROIs) were defined and average ΔF values within a given ROI were plotted versus time. Unless otherwise stated, statistical values are means ± SD. Student's *t*-test was used for statistical comparisons of two sample populations, and ANOVA was used when more than two sample populations are compared. All statistical tests were performed using Origin 2015 (OriginLab, Northampton, MA).

RESULTS

Oscillatory activity in acute slices, brain stem slice cultures, and brain stem-cerebellar cocultures. Bilateral oscillatory calcium activity was detected in fluo-8 AM-loaded brain stem slices that expose the preBötC at their rostral surface (Ruangkittisakul et al. 2011, 2014) and was subsequently imaged both acutely and after 7–28 days in vitro (DIV) using the Stoppini culturing method (Fig. 1, *A* and *B*). In both acute slices and cultures, synchronized calcium activity was observed in an inverted V-shaped pattern with signals concentrated in dorsal (Fig. 1, *A* and *B*, blue circles) and ventral oscillatory groups (Fig. 1, *A* and *B*, red circles). Acute slices showed respiratory-related rhythmic activity at 10.9 ± 4.2 bursts/min (n = 10), and slices maintained in organotypic culture for 7–22 DIV oscillated at 13.7 ± 10.6 bursts/min (n = 15). When we cocultured the brain stem slice with two cerebellar slice explants (placed along either the dorsolateral or ventrolateral border of the slice), then the rhythm was faster (22.4 ± 8.3 bursts/min, n = 26; Fig. 1, *C* and *D*; Supplemental Video S1, available in the data supplement online at the *Journal of Neurophysiology* Web site). Brain stem-cerebellar cocultures (7–43 DIV) were faster than both acute slices and brain stem slice cultures, and there was no significant linear correlation or other obvious relationship between DIV and burst frequency (not shown; linear correlation coefficient r = 0.1, n = 19). Preparation type had a significant effect on frequency [$F(2,48)$ = 8.9, P = 0.0005; Fig. 1*D*, *left*]. Post hoc comparison using Bonferroni or Tukey tests indicate that coculture oscillation frequency is significantly different from that in brain stem slice cultures (mean difference = 8.7 bursts/min, P = 0.008) and acute slices (mean difference = 11.5 bursts/min, P = 0.002).

Calcium transients in brain stem slice cultures were longer lasting and had a slower onset compared with acute slices or brain stem-cerebellar cocultures. The mean burst duration of calcium activity in the ventral oscillatory group of brain stem slice cultures measured 785 ± 257 ms (n = 13) compared with 367 ± 59 ms in acute slice preparations (n = 10) and 514 ± 169 ms in cocultures (n = 26). Preparation type had a significant effect on burst duration [$F(2,46) = 16.2$, $P = 4.7 \times 10^{-6}$; Fig. 1*D*, *middle*]. Post hoc comparison tests indicate that brain stem slice culture burst duration is significantly different from that in both acute slices (mean difference = 418 ms, $P = 6.1 \times 10^{-6}$) and cocultures (mean difference = 272 ms, P = 0.0002).

The rate of signal onset, measured as the 10–90% rise time above baseline fluorescence, was slower in brain stem slice cultures (375 ± 213 ms, n = 13) compared with acute slice preparations (226 ± 43 ms, n = 10) and cocultures (223 ± 57 ms, n = 26). Preparation type had a significant effect on signal onset [$F(2,46)$ = 7.8, P = 0.001; Fig. 1*D*, *right*], and post hoc comparison tests indicate that burst rise time in brain stem slice culture is significantly different from that in both acute slices (mean difference = 149 ms, P = 0.01) and cocultures (mean difference = 152 ms, P = 0.001).

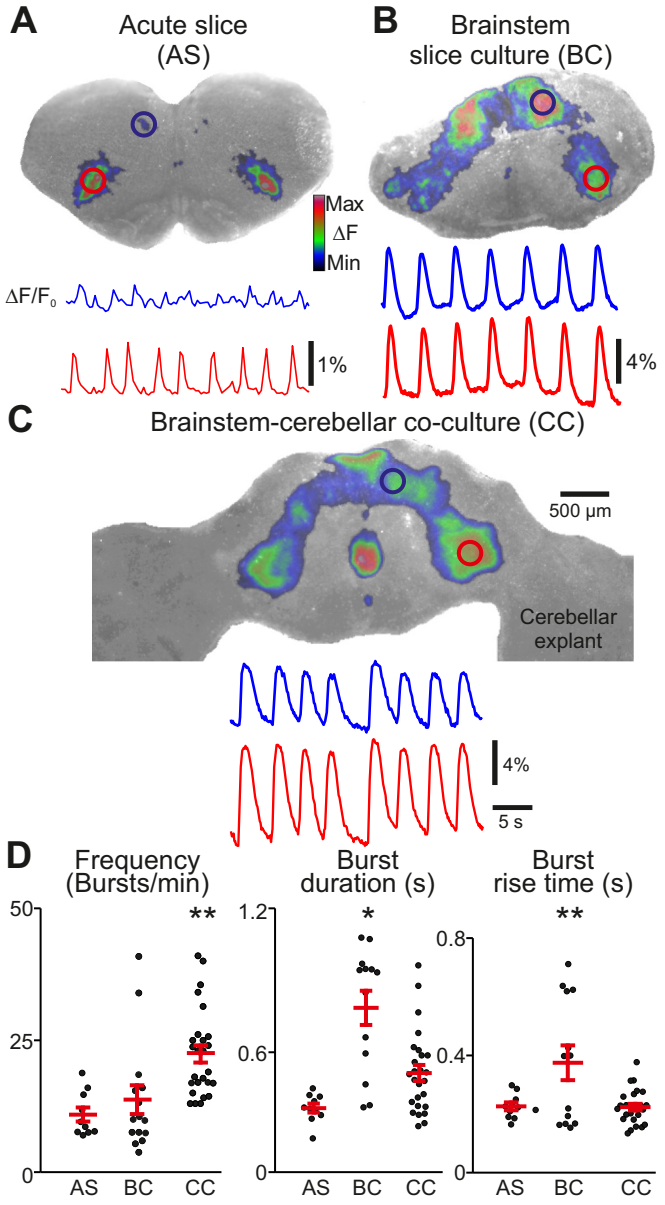

Fig. 1. Oscillatory calcium activity in 3 different transverse brain stem slice preparations. *A, top*: cycle-triggered average of fluorescent calcium activity overlaid on brightfield image of an acute slice preparation (AS; for anatomical reference). Regions of interest (ROIs) are drawn over rhythmically active areas at ventrolateral (red) and dorsomedial regions (blue). *Bottom*, change in fluorescence over baseline fluorescence intensity ($\Delta F/F_0$) traces of rhythmic activity. Blue trace corresponds to dorsomedial ROI; red trace corresponds to ventrolateral ROI. *B* and *C*: same conventions as in *A* but showing calcium activity from a brain stem slice culture (BC) and a brain stem-cerebellar coculture preparation (CC), respectively. The color calibration scale in *A* shows the colors associated with the ΔF range from minimal to maximal and applies to all plots in figures showing ΔF images. *D*: graphs showing burst frequency, burst duration (half-width; taken at 50% from baseline), and burst rise time (10–90% amplitude from baseline). Error bars show means ± SE. $^*P < 0.05$; $^{**}P < 0.001$ (ANOVA with post hoc comparison using Tukey tests). Note that the burst frequency is higher in CC preparations vs. AS and BC cultures. Also, the difference in burst duration and rise time between AS and CC preparations is not significant.

The signal-to-noise ratio was higher in cocultured preparations compared with acute slices. Under similar dye-loading

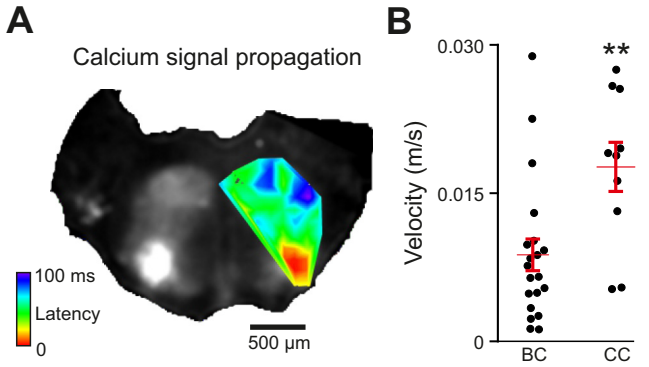

Fig. 2. Propagation of calcium activity in brain stem slice cultures and brain stem-cerebellar cocultures. *A*: time series *Z* projection of maximum fluorescent calcium activity in a brain stem-cerebellar coculture. The heat map overlay shows threshold signal increases from low (red) to high latencies (blue) during a single rhythmic burst acquired at 129 frames/s. *B*: average velocity of signal propagation in BC vs. CC preparations. Error bars indicate means ± SE. $^{**}P < 0.001$ (Student's *t*-test).

and imaging conditions, peak calcium signals from the center of the ventral oscillatory group measured 340% higher in magnitude in cocultured preparations (5.5 ± 3.3%, $n = 8$) and 550% higher in brain stem slice culture preparations (8.8 ± 3.1%, $n = 8$) compared with acute preparations [1.6 ± 0.7%, $n = 8$; $F(2,21) = 14.8$, $P = 9.6 \times 10^{-5}$]. Active areas whose calcium activity was not normally visible in acute slices also became apparent in cultured preparations. In 53% ($n = 34$) of all cultured preparations, midline activity between ventral oscillatory groups was detectable.

We also prepared brain stem slices cocultured with cerebellar explants using roller-drum methods (Gahwiler 1981), and these cultures (17–19 DIV) also showed spontaneous oscillatory activity, with a burst frequency of 28.6 ± 5.9 bursts/min, burst duration of 625 ± 97 ms, and 10–90% rise time of 269 ± 29 ms. These characteristic measurements were not significantly different from those of similar Stoppini-type cocultures ($P = 0.09–0.16$, $n = 5$).

Spread of activity in brain stem slice cultures and brain stem-cerebellar cocultures. Both brain stem slice cultures and brain stem-cerebellar cocultures display oscillatory calcium burst patterns that propagate ipsilaterally, traveling from their point of initiation in the ventrolateral area toward the dorsomedial border at varying velocities (Fig. 2*A*). When imaged at 129 Hz, the signal in brain stem-cerebellar cocultures propagated 275% as fast (0.022 ± 0.007 m/s, $n = 8$) as that in brain stem slice cultures (0.008 ± 0.005 m/s, $n = 9$, $P < 0.001$; Fig. 2*B*). In each slice there was a detectable latency in the signal rise between contralateral ventral oscillatory groups. In every case, for both brain stem slice cultures and brain stem-cerebellar cocultures, calcium signals took longer to propagate from ventral to dorsal regions than to contralaterally equivalent regions, where the activity appeared within 1–2 frames, which made it too uncertain to calculate a precise velocity or possible dominant or alternating initiation site ($n = 7$). Thus, regardless of preparation type, synchronized bursts first occurred bilaterally between contralateral ventral oscillatory groups and then propagated more slowly in the dorsomedial direction.

Ventral oscillatory group activity in multiple neurons and calcium transients in dendritic profiles. In acute slice preparations, calcium and voltage dye fluorescence imaging often appears as diffuse regional fluorescence due to light scattering in the tissue, or instead captures only a subset of rhythmically active neurons within the field of view or focal plane (Funk and Greer 2013; Koshiya and Smith 1999; Koshiya et al. 2014; Onimaru and Homma 2003). Similarly, live imaging of dendritic processes at the cellular level, even with the aid of two-photon and confocal imaging, can be difficult due to branching in the *Z*-axis and increased light scattering at locations deep within the slice (Del Negro et al. 2011; Funk and Greer 2013; Katona et al. 2011). One advantage of culturing brain slices is the reduced thickness compared with acute slices (Stoppini et al. 1991). Using the Stoppini culturing method, we reduced the thickness of the brain stem slices cultured to 104 ± 31 μm (measured in sagittal sections of Epon-embedded 7–31 DIV oscillating cultures, $n = 5$) from a thickness of 400 μm in the acute slices at 0 DIV. The dorsal-to-ventral distance at the slice midline increased to 1,943 ± 183 μm compared with 1,490 ± 74 μm in acute slices acquired from age-matched controls (postnatal day 2.5; $P < 0.05$, $n = 5$). Thus the cultures flatten out and the reduced thickness made it possible to record synchronized calcium transients from hundreds of neurons in the same focal plane (Fig. 3, *A* and *B*). At higher magnification, both somatic and proximal (~100 μm) dendritic activity could be recorded in fluo-8 AM-loaded neurons (Fig. 3*C*; Supplemental Video S2).

Retrograde biocytin labeling in roller-drum cultures. The preBötC contains commissural interneurons, which synchronize bilateral halves of the preBötC, as well as interneurons that project ipsilaterally to premotor neurons in the intermediate reticular formation as well as hypoglossal motor neuron pools (Wang et al. 2014). If the inverted V-shaped pattern of rhythmic calcium activity in cultures corresponds to that seen in acute slices, then similar axon projections ought to be

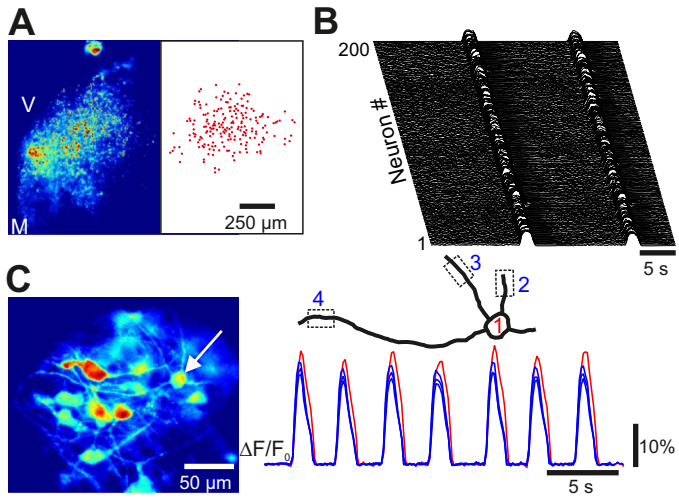

Fig. 3. Low- and high-magnification views of oscillatory activity. *A, left*: oscillatory calcium activity in the ventral oscillatory group at low magnification using ×10 objective (*Z* projection of standard deviation from 200-frame image stack at 10 Hz; V, ventral; M, medial). *Right*, position of 200 oscillating cell body ROIs from the image at *left*. *B*: waterfall diagram of $\Delta F/F_0$ traces from the 200 ROIs shown in *A*. Note the tight synchronization during 2 cycles. *C, left*: cycle-triggered average of oscillatory calcium activity at high magnification using a ×63 objective. Note the visualization of somas and dendritic profiles. *Right*, reconstruction of the soma-dendritic territory from 1 neuron and the associated $\Delta F/F_0$ traces from 3 dendritic and 1 somatic ROI (indicated by dotted squares).

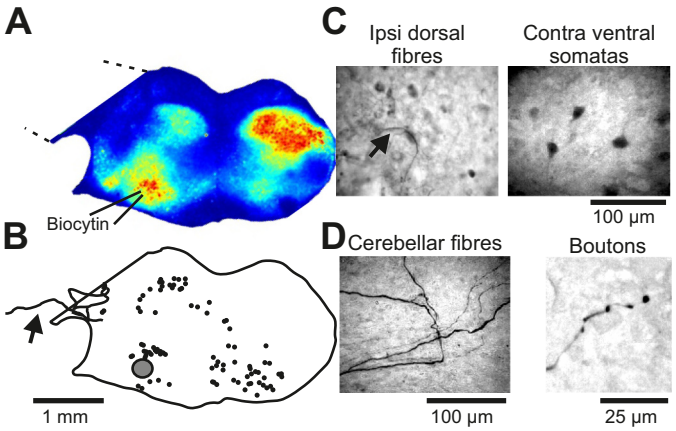

Fig. 4. Retrograde labeling of neurons following local co-iontophoresis of biocytin and KCl in roller-drum cultures. *A*: oscillatory calcium activity (*Z* projection of standard deviation from 300-frame image stack) in a roller-drum brain stem-cerebellar coculture. *B*: camera lucida reconstruction of the position of retrogradely labeled neurons (solid circles) after local co-iontophoresis at the ventral oscillatory group (shaded circle). Note that some labeled fibers cross into the cerebellar explant (arrow). *C*: photomicrograph of labeled fibers located in the ipsilateral dorsal part, and somata in the contralateral ventral part, of the coculture. *D*: photomicrograph of labeled fibers entering the cerebellar part of the cultures and ending in boutons.

maintained in the cultured preparation. To test this prediction, we electroporated 1% biocytin using patch pipettes placed in the ventral oscillatory group of Roller-drum cultures ($n = 3$). Retrogradely labeled neurons were located around the injection site; somata and projecting fibers were found in the ipsilateral dorsal part of the culture, at the midline, and in the contralateral ventrolateral part of the cultures (Fig. 4, *B* and *C*). The somatic positions of the labeled neurons and fibers corresponded to oscillatory regions recorded before electroporation (Fig. 4, A and *B*). The biocytin labeling suggests that the pattern of activity in cultures is attributable to an underlying bilateral network of neurons in the preBötC, which also project dorsally, presumably to premotor and motor-related respiratory neural circuits. Biocytin-labeled fibers entering the cerebellar explant, terminating in bouton-like structures, were detected in one slice coculture (Fig. 4, *B* and *D*), indicating a degree of synaptic interconnectivity between the brain stem and cerebellar neurons.

Calcium activity in GFAP-labeled cells. Oscillatory calcium transients have been reported in astrocytes in sync with neighboring preBötC neurons (Oku et al. 2015). We tested for rhythmic glial activity in brain stem-cerebellar cocultures prepared from transgenic mice that express EGFP coupled to GFAP (Fig. 5). However, oscillatory calcium fluorescence was undetectable in 98% ($n = 288$, 10 cultures) of the recorded GFAP$^+$ cells (Fig. 5*A*). A few EGFP-expressing astrocytes ($n = 5$) generated one-time calcium transients independently of calcium transients in neighboring oscillating neurons (Fig. 5*B*, $n = 4$). The mean rise-time of these transient events (810 ± 235 ms, $n = 5$) exceeded the length of calcium transients in neighboring rhythmic neurons (393 ± 66 ms; $n = 119$ neurons across 5 cultures, $P = 0.0051$). Half-width duration of transients in GFAP$^+$ cells (1,028 ± 124 ms) was 24% longer than in rhythmic neurons (866 ± 31 ms; $n = 119$ cells across 5 cultures, $P = 0.022$).

Whole cell electrophysiology. To assess whether neuronal behavior in cultures resembles preBötC neurons in acute slice preparations (Funk and Greer 2013), we recorded the voltage trajectory in rhythmic neurons from culture preparations. First, using calcium imaging, rhythmically active cells within the ventral oscillatory group were targeted for whole cell patch-clamp recordings (Fig. 6*A*; $n = 10$). Rhythmic drive potentials (duration 343 ± 207 ms, $n = 7$) that reflect underlying network activity were recorded at typical membrane potential (overriding action potentials were removed via bandpass filtering) and at hyperpolarized potentials by using negative bias current to uncover nonlinear membrane behavior indicative of recruitment of active conductances (Fig. 6*B*). The amplitude of the underlying drive potential was 185% larger in rhythmic neurons held at close to resting membrane potential (19.0 ± 6.6 mV; $n = 7$) than in neurons held at membrane potentials below the threshold of action potential generation during the burst (10.3 ± 3.7 mV; $n = 5$, $P < 0.05$).

Finally, we tested pharmacological modulation of burst frequency by neuropeptides. From a control frequency of 24.4 ± 6.4 bursts/min, the NK1-receptor agonist SP (500 nM) sped up the frequency by 134% to 32.7 ± 9.3 bursts/min ($P < 0.05$), and adding the μ-opioid agonist DAMGO (1 μM) on top of SP slowed the frequency by 50% to 16.5 ± 8.7 bursts/min ($P < 0.01$, $n = 6$ cumulative dosings; Fig. 6*C*).

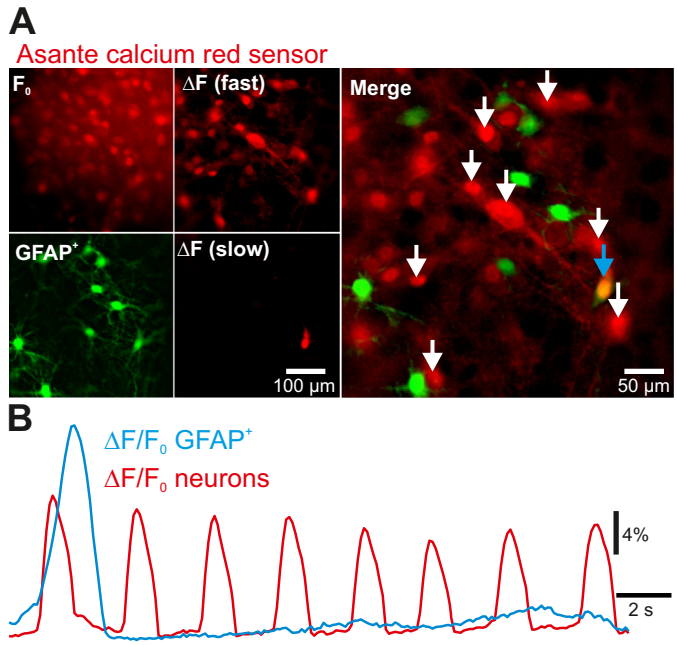

Fig. 5. Simultaneous imaging of glial fibrillary acidic protein-labeled (GFAP$^+$) cells expressing enhanced green fluorescent protein (EGFP; green channel) and time series of fluorescent calcium activity (red channel). *A*, *top left*: baseline calcium (F_0) with a cycle-triggered average of calcium fluorescence taken between rhythmic events. *Bottom left*, expression of EGFP in GFAP$^+$ cells in the same field of view. *Top center*, cycle-triggered average of maximum calcium fluorescence during fast rhythmic burst events [ΔF (fast)] minus baseline fluorescence. *Bottom center*, *Z*-projection sum of $\Delta F/F_0$ across $t = 0.7$–3.2 s showing a slow independent calcium transient [ΔF (slow)]. *Right*, merge of EGFP expression, cycle-triggered average maxima, and the *Z*-projection sum of the slow calcium transient; overlap between green and red channels is shown at the blue arrow. *B*: $\Delta F/F_0$ plot of rhythmic neuronal calcium activity (red) vs. GFAP$^+$-associated calcium activity (blue). Neuronal activity was averaged from 8 ROIs indicated by white arrows in *A*. GFAP$^+$ ROI is indicated by the blue arrow.

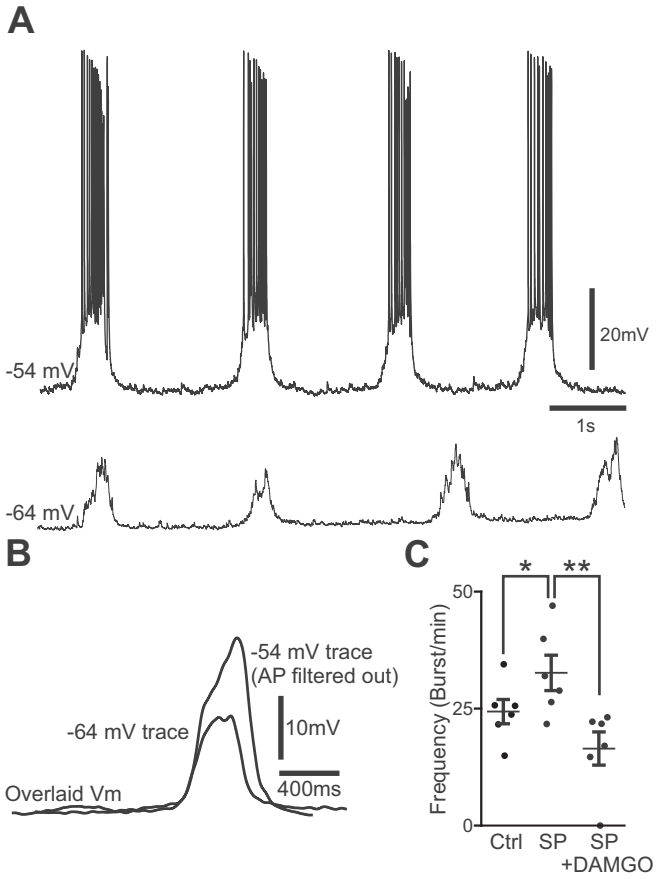

Fig. 6. Whole cell patch-clamp recordings from a rhythmically active neuron in the ventral oscillatory group of a brain stem-cerebellar coculture after 7 days in vitro. *A*, *top* trace: normal bursting activity at resting membrane potential (V_m) with zero current bias applied. *Bottom* trace, rhythmic drive potential at a hyperpolarized potential after negative bias (−0.1 nA) was applied. *B*: overlaid cycle-triggered and action potential-filtered average traces of the burst events occurring in *A*. Note that the underlying burst envelope is larger in amplitude at resting V_m levels. *C*: modulation of burst frequency by 500 nM substance P (SP) and 500 nM SP + 1 μM [D-Ala^2, N-Me-Phe^4, Gly^5-ol]-enkephalin acetate salt (DAMGO). Error bars indicate means ± SE ($n = 6$). *$P < 0.05$, control (Ctrl) vs. SP. **$P < 0.001$, SP vs. SP + DAMGO (paired-sample *t*-tests).

DISCUSSION

Acute slice preparations containing the preBötC survive in organotypic culture conditions and maintain patterned rhythmic calcium activity, which we attribute to underlying neuronal inspiratory-like drive potentials and spike bursts in constituent preBötC interneurons. Bursts in culture began with fast bilateral coactivation in ventrolateral regions of the slice and then propagated ipsilaterally to the dorsomedial regions of the culture preparations. The inverted V-shaped activity pattern was consistent; it did not depend on the presence of cerebellar explants. The ipsilateral ventral-to-dorsal propagation velocity was on the order of 0.02 m/s in brain stem-cerebellar slice cultures. This velocity is roughly 10 times slower than a published value of 0.24 m/s in the commissural fiber tracts connecting bilateral preBötC in rhythmically active acute slices of neonatal rats using voltage imaging (Koshiya et al. 2014). Thus the slice cultures appear to generate patterned activity that spreads dorsally slower than the normal velocity of fine axons abundant in the neonatal central nervous system (Sternberger et al. 1979), which may imply that the activity is shaped by local synaptic processes in networks of neurons. The pattern also overlaps the expression of cells, in the transverse plane of the brain stem and cervical spinal cord, derived from the homeodomain transcription factor Dbx1, which gives rise to rhythmogenic interneurons that comprise the preBötC (Bouvier et al. 2010; Gray et al. 2010; Picardo et al. 2013) and also play a role in premotor drive transmission (Wang et al. 2014).

In some recordings we also observed midline activity, which may reflect raphe neurons that interconnect with the preBötC and increase firing frequency in response to rhythmic preBötC input (Ptak et al. 2009). Retrograde biocytin labeling from the ventral oscillatory group revealed projections in both the contralateral ventral oscillatory group and dorsomedial regions, similar to that obtained via in vivo fluoro gold injection into the preBötC (Koshiya et al. 2014). Retrogradely labeled neurons were also found in the midline, further suggesting the involvement of raphe neurons. Thus it appears unlikely that rhythmic calcium changes in the slice occur due to spontaneous calcium oscillations, but rather they resemble the neuronal behavior found in acute slices, similar in both dynamics and patterning, and occurring over anatomic regions that correspond to known areas of activity and to locations of cells vital for production of the respiratory rhythm. The presence of cerebellar explants cocultured with preBötC slices bolsters the rhythm, causing it to oscillate faster than acute preBötC preparations, but with similar burst duration and 10–90% rise times. Without the addition of cerebellar explants, brain stem cultures oscillate at the same frequency as acute preparations, but individual bursts have a slower onset and offset: increased burst duration and rise time. Although the specific roles of cerebellar explants that promote preBötC-like rhythmic activity in cultures are unknown, spontaneous oscillatory activity in cerebellar granule cells may contribute to the overall excitability of the slice (Apuschkin et al. 2013; De Zeeuw et al. 2008), especially if coculturing allows granule cell axon entry into the preBötC and facilitates excitatory synaptic connections with preBötC interneurons of the ventral oscillatory group. Since preBötC-like rhythmic behavior occurred in the absence of cerebellar explants but these rhythms were faster with cerebellar cocultures, we conclude that cerebellar circuits augment excitability in the cultured preBötC but do not contribute to the cellular mechanisms underlying rhythm generation.

Because of gradual thinning of the slice and consequent reduction of light scattering in the tissue over time, the brain stem slice culture preparation allows for higher spatial resolution during imaging at both the cellular and network level and greater amplitude of fluorescent signals. This could be advantageous for analyzing larger portions of rhythmically active cell populations in the preBötC and adjacent premotor areas than has previously been possible in acute slices. For example, the culture preparation we characterize in this report may facilitate real-time visualization and perturbation of individual burst percolation across the rhythmogenic core and into premotor areas. Our preparation makes it feasible to stimulate and record large populations (approximately hundreds of neurons), since neighboring somata that would otherwise be spread through the *Z*-axis become coplanar (or nearly so for practical purposes). These conditions also simplify imaging requirements: population-level recordings could be acquired using wide-field excitation. Additionally, subcellular sections of neurons (e.g., dendritic processes) could be visualized at higher

magnifications. Therefore, it is more likely that regions of dendritic processes several hundred microns in size could be captured in a single focal plane, and thus intercellular signal propagation arising from recurrent excitation along the dendritic arborizations of rhythmic neurons, as well as its impact on burst generation, might also be more readily visualized.

Astrocytes have been implicated in respiratory rhythm generation (Hartel et al. 2009; Hulsmann et al. 2000; Oku et al. 2015; Schnell et al. 2011). We tested for the presence of calcium oscillations in the astrocytes of brain stem-cerebellar cocultures. We were able to image a large number of cells simultaneously using conventional wide-field illumination microscopy. We used a bath-applied red-shifted calcium indicator, despite an inherently reduced fluorescence intensity compared with brighter green dyes (e.g., Oregon green BAPTA 1, fluo 8), because of the flattened state and reduced tortuosity in the culture preparation. There was no apparent preinspiratory activity or oscillatory activity in 288 recorded $GFAP^+$ cells. However, we cannot entirely rule out low-amplitude calcium oscillations. Previous recordings from astrocytes in preBötC brain stem slices employed the high-affinity indicator Oregon green BAPTA 1 (K_d = 170 nM), whereas we used the medium-affinity indicator Asante calcium red (K_d = 400 nM). Previously reported astrocytic fluctuations were of small amplitude ($<1\%$ $\Delta F/F_0$) and only visible after filtering (Oku et al. 2015). It is therefore plausible that we failed to detect astrocytic fluctuations due to experimental limitations related to our green GFAP reporter strain coupled with a red calcium dye of limited sensitivity. Furthermore, the tight proximity of cell layers in culture conveniently allows many cells to be recorded simultaneously with less light scattering due to tissue thickness, but the signal is likewise prone to contamination by neuronal activity that is marginally out of focus yet still of a greater magnitude than any glial signals, which may be especially true at higher magnification. Finally, it is possible that astrocytes in this case were inadequately labeled due to loading feasibility of the indicator dye or that they simply behaved differently in a culture environment.

Whole cell electrophysiology data show neurons in the ventral oscillatory group of brain stem-cerebellar cocultures whose behavior appears similar to previously described rhythmic neurons in the preBötC of acute slices (Funk and Greer 2013; Ramirez et al. 2012). These neurons receive periodic inspiratory drive potentials that generally produce bursts of action potentials with an underlying burst envelope that is larger at rest than at hyperpolarized potentials (Fig. 6*B*), suggesting that voltage- or calcium-dependent conductances amplify the synaptic drive (Ramirez et al. 2012). The drive potentials had a duration of ~350 ms, which compares to the ~870-ms half-amplitude duration of the calcium signal in individual neurons, illustrating that the shape and time course of the calcium signal also depend on cellular calcium kinetics. Taking these findings in conjunction with calcium imaging data and retrograde tracing with biocytin, we conclude that organotypic cultures retain a rhythmically active ventral network that corresponds to the preBötC. Its activity pattern spans dorsally into regions such as the intermediate reticular formation, the nucleus tractor solitarius, and the XII nucleus, which are associated with premotor and motor circuits that serve respiration. Midline activity also appears to correspond with the raphe obscurus (Ptak et al. 2009). Decreased tissue thickness, and consequently the ability to capture many active neurons in the same focal plane with significantly reduced fluorescence scattering, likely accounts for the increase in signal amplitude in cultures (both brain stem slice cultures and brain stem-cerebellar cocultures) compared with acute slices. However, the existence of rhythmic neurons in the ventrolateral slice culture, and in adjacent dorsomedial regions, does not necessarily guarantee that these neurons correspond one-to-one to preBötC interneurons and respiratory premotor or motor neurons, or that they have not modified their behavior or physiology in some way. A degree of synaptic remodeling certainly occurs over time in vitro: we can see promiscuous fibers projecting between cerebellar and brain stem explants via retrograde biocytin tracing. Thus we cannot exclude the possibility that circuits not found in the intact animal or unnatural strengthening of existing circuits develops over time in the cultures, which certainly should be taken into consideration when using this preparation. However, general synaptic connectivity between contralateral and dorsomedial motor regions of the slice appears to be preserved, and more importantly, the calcium activity in preBötC cultures reflects a consistent rhythmic pattern initiation in the ventral oscillatory group followed by fast bilateral synchronization and subsequent propagation of signal to dorsomedial regions. Pharmacological modulation of the rhythm using agonists for NK1 and μ-opioid receptors also mimics responses seen in acute slice (Gray et al. 1999), demonstrating that essential peptidergic modulating systems are intact in the cultures, at least at the postsynaptic level.

Thus the preBötC slice culture preparation could be a useful model of respiratory rhythm generation that approximates the already widely used acute slice preparation and is amenable for optical and electrical stimulation and recording. The longevity of the culture preparation will facilitate molecular biological experiments and techniques, as well as any protocol that requires pharmacological perturbations lasting multiple days or weeks.

ACKNOWLEDGMENTS

We thank Morten Bjerre Nielsen for technical assistance.

GRANTS

This work was supported by The Danish Research Council, The Lundbeck Foundation, Mindefonden for Alice Brenaa, Den Owensenke Fond, Lægeforeningens forskningsfond, Agnes og Pouls Friis Fond, Fonden til Lægevidenskabens Fremme, and Brødrene Hartmans Fond, as well as National Institutes of Health Grants R21 NS087257 (to C. A. Del Negro) and R01 HL104127 (to C. A. Del Negro).

DISCLOSURES

No conflicts of interest, financial or otherwise, are declared by the authors.

AUTHOR CONTRIBUTIONS

W.S.P., M.H., C.A.D.N., and J.C.R. conception and design of research; W.S.P., M.H., and J.C.R. performed experiments; W.S.P., M.H., C.A.D.N., and J.C.R. analyzed data; W.S.P., M.H., C.A.D.N., and J.C.R. interpreted results of experiments; W.S.P., C.A.D.N., and J.C.R. prepared figures; W.S.P., C.A.D.N., and J.C.R. drafted manuscript; W.S.P., M.H., C.A.D.N., and J.C.R. edited and revised manuscript; W.S.P., M.H., C.A.D.N., and J.C.R. approved final version of manuscript.

REFERENCES

Apuschkin M, Ougaard M, Rekling JC. Spontaneous calcium waves in granule cells in cerebellar slice cultures. *Neurosci Lett* 553: 78–83, 2013.

Bouvier J, Thoby-Brisson M, Renier N, Dubreuil V, Ericson J, Champagnat J, Pierani A, Chedotal A, Fortin G. Hindbrain interneurons and axon guidance signaling critical for breathing. *Nat Neurosci* 13: 1066–1074, 2010.

De Zeeuw CI, Hoebeek FE, Schonewille M. Causes and consequences of oscillations in the cerebellar cortex. *Neuron* 58: 655–658, 2008.

Del Negro CA, Hayes JA, Rekling JC. Dendritic calcium activity precedes inspiratory bursts in preBotzinger complex neurons. *J Neurosci* 31: 1017–1022, 2011.

Feldman JL, Del Negro CA, Gray PA. Understanding the rhythm of breathing: so near, yet so far. *Annu Rev Physiol* 75: 423–452, 2013.

Funk GD, Greer JJ. The rhythmic, transverse medullary slice preparation in respiratory neurobiology: contributions and caveats. *Respir Physiol Neurobiol* 186: 236–253, 2013.

Gahwiler BH. Organotypic monolayer cultures of nervous tissue. *J Neurosci Methods* 4: 329–342, 1981.

Gray PA, Hayes JA, Ling GY, Llona I, Tupal S, Picardo MC, Ross SE, Hirata T, Corbin JG, Eugenin J, Del Negro CA. Developmental origin of preBotzinger complex respiratory neurons. *J Neurosci* 30: 14883–14895, 2010.

Gray PA, Rekling JC, Bocchiaro CM, Feldman JL. Modulation of respiratory frequency by peptidergic input to rhythmogenic neurons in the preBotzinger complex. *Science* 286: 1566–1568, 1999.

Hartel K, Schnell C, Hulsmann S. Astrocytic calcium signals induced by neuromodulators via functional metabotropic receptors in the ventral respiratory group of neonatal mice. *Glia* 57: 815–827, 2009.

Hartelt N, Skorova E, Manzke T, Suhr M, Mironova L, Kugler S, Mironov SL. Imaging of respiratory network topology in living brainstem slices. *Mol Cell Neurosci* 37: 425–431, 2008.

Hulsmann S, Oku Y, Zhang W, Richter DW. Metabolic coupling between glia and neurons is necessary for maintaining respiratory activity in transverse medullary slices of neonatal mouse. *Eur J Neurosci* 12: 856–862, 2000.

Katona G, Kaszas A, Turi GF, Hajos N, Tamas G, Vizi ES, Rozsa B. Roller coaster scanning reveals spontaneous triggering of dendritic spikes in CA1 interneurons. *Proc Natl Acad Sci USA* 108: 2148–2153, 2011.

Koshiya N, Oku Y, Yokota S, Oyamada Y, Yasui Y, Okada Y. Anatomical and functional pathways of rhythmogenic inspiratory premotor information flow originating in the pre-Botzinger complex in the rat medulla. *Neuroscience* 268: 194–211, 2014.

Koshiya N, Smith JC. Neuronal pacemaker for breathing visualized in vitro. *Nature* 400: 360–363, 1999.

Lalo U, Pankratov Y, Kirchhoff F, North RA, Verkhratsky A. NMDA receptors mediate neuron-to-glia signaling in mouse cortical astrocytes. *J Neurosci* 26: 2673–2683, 2006.

Manzini I, Schweer TS, Schild D. Improved fluorescent (calcium indicator) dye uptake in brain slices by blocking multidrug resistance transporters. *J Neurosci Methods* 167: 140–147, 2008.

Oku Y, Fresemann J, Miwakeichi F, Hulsmann S. Respiratory calcium fluctuations in low-frequency oscillating astrocytes in the pre-Botzinger complex. *Respir Physiol Neurobiol*. First published March 5, 2015; doi: 10.1016/j.resp.2015.02.002.

Onimaru H, Homma I. A novel functional neuron group for respiratory rhythm generation in the ventral medulla. *J Neurosci* 23: 1478–1486, 2003.

Picardo MC, Weragalaarachchi KT, Akins VT, Del Negro CA. Physiological and morphological properties of Dbx1-derived respiratory neurons in the pre-Botzinger complex of neonatal mice. *J Physiol* 591: 2687–2703, 2013.

Ptak K, Yamanishi T, Aungst J, Milescu LS, Zhang R, Richerson GB, Smith JC. Raphe neurons stimulate respiratory circuit activity by multiple mechanisms via endogenously released serotonin and substance P. *J Neurosci* 29: 3720–3737, 2009.

Ramirez JM, Doi A, Garcia AJ III, Elsen FP, Koch H, Wei AD. The cellular building blocks of breathing. *Compr Physiol* 2: 2683–2731, 2012.

Ruangkittisakul A, Kottick A, Picardo MC, Ballanyi K, Del Negro CA. Identification of the pre-Botzinger complex inspiratory center in calibrated "sandwich" slices from newborn mice with fluorescent Dbx1 interneurons. *Physiol Rep* 2: e12111, 2014.

Ruangkittisakul A, Panaitescu B, Ballanyi K. K^+ and Ca^{2+} dependence of inspiratory-related rhythm in novel "calibrated" mouse brainstem slices. *Respir Physiol Neurobiol* 175: 37–48, 2011.

Schneider CA, Rasband WS, Eliceiri KW. NIH Image to ImageJ: 25 years of image analysis. *Nat Methods* 9: 671–675, 2012.

Schnell C, Fresemann J, Hulsmann S. Determinants of functional coupling between astrocytes and respiratory neurons in the pre-Botzinger complex. *PLoS One* 6: e26309, 2011.

Smith JC, Ellenberger HH, Ballanyi K, Richter DW, Feldman JL. Pre-Botzinger complex: a brainstem region that may generate respiratory rhythm in mammals. *Science* 254: 726–729, 1991.

Sternberger NH, Quarles RH, Itoyama Y, Webster HD. Myelin-associated glycoprotein demonstrated immunocytochemically in myelin and myelin-forming cells of developing rat. *Proc Natl Acad Sci USA* 76: 1510–1514, 1979.

Stoppini L, Buchs PA, Muller D. A simple method for organotypic cultures of nervous tissue. *J Neurosci Methods* 37: 173–182, 1991.

Wang X, Hayes JA, Revill AL, Song H, Kottick A, Vann NC, LaMar MD, Picardo MC, Akins VT, Funk GD, Del Negro CA. Laser ablation of Dbx1 neurons in the pre-Botzinger complex stops inspiratory rhythm and impairs output in neonatal mice. *Elife* 3: e03427, 2014.